Solution-Processed Small Molecules Using Different Electron Linkers for High-Performance Solar Cells

ARTICLE *in* ADVANCED MATERIALS · SEPTEMBER 2013

Impact Factor: 17.49 · DOI: 10.1002/adma.201301716 · Source: PubMed

7 AUTHORS, INCLUDING:

Yongsheng Liu
University of California, Los Angeles
48 PUBLICATIONS **3,927** CITATIONS
SEE PROFILE

Letian Dou
UC Berkeley; Lawrence Berkeley National L…
31 PUBLICATIONS **3,830** CITATIONS
SEE PROFILE

Ziruo Hong
University of California, Los Angeles
129 PUBLICATIONS **7,612** CITATIONS
SEE PROFILE

Gang Li
University of California, Los Angeles
143 PUBLICATIONS **23,200** CITATIONS
SEE PROFILE

Solution-Processed Small Molecules Using Different Electron Linkers for High-Performance Solar Cells

*Yongsheng Liu, Yang (Michael) Yang, Chun-Chao Chen, Qi Chen, Letian Dou, Ziruo Hong, Gang Li, and Yang Yang**

Solution processed organic solar cells (OSCs) have been intensively investigated over the past decade due to their potential application in the low-cost fabrication of large-area, flexible, and lightweight devices.[1] Significant progress has been made in this field, and the power conversion efficiencies (PCEs) of polymer solar cells have reached over 10% both in single junction and tandem devices, primarily due to the development of new donor materials and interface layers as well as advances in device engineering.[2] In parallel with polymer donor materials, recently, bulk heterojunction (BHJ) OSCs based on solution-processed small molecules as donors have attracted increasing attention.[3] The advantages of small molecule donors include well-defined molecular structures, high purity without batch-to-batch variation, high carrier mobilities, and absence of end group contaminants. To date, the efficiency of solution processed small molecule OSC has reached 7%,[4] making these materials ideal candidates for solution processed OSCs. While high external quantum efficiency (EQE) and respectable open circuit voltage (V_{oc}) have been achieved, one of the limiting factors for the PCE of small molecule OSCs, in comparison with their polymeric counterparts, is the fill factor (FF), typically <50%.[3b,3c,5] It has been known that moderate phase separation in the donor:fullerene blend films is necessary to facilitate charge transport and collection.[1a] However, the conjugated small molecules and fullerene derivatives tend to form films with amorphous nature.[3a–c] The non-geminate recombination dominates the shunt resistance of the devices mainly because of inferior carrier mobilities, resulting in low FF.[6] Therefore, it is important to use donor materials that exhibit good miscibility with acceptor materials and maintain sufficient crystallinity, in order to induce nanoscale phase separation between donor and acceptor. Hence, to improve the FF and photovoltaic performance, it is necessary to design and synthesize new molecules with good miscibility with the acceptor materials and thus good film quality, broad and efficient optical absorption, matched energy levels, and high charge carrier mobility.

The oligothiophenes with six thiophene units are among the most investigated oligomers, and exhibit excellent hole mobilities. For example, α,ω-didecyl-sexithiophene exhibits a FET mobility as high as ≈0.5 $cm^2\ V^{-1}s^{-1}$.[7] For solution processed OSCs, it requires proper side chains on the conjugated backbone to achieve solubility and other desired properties. However, saturated alkyl chains do not contribute to the charge transport, and often cause the conjugated backbone to twist, which reduces the conjugation length and consequently increases the optical bandgap.[8] Designing and controlling the position and density of the alkyl side chains are critical for good solubility of materials, and to improve molecular packing[9] and solid-state miscibility with fullerenes. In order to compensate the negative effects of side chains, introducing an electron linker to the conjugated main chains is also effective in maintaining a co-planar structure, and releasing the distortion induced by the alkyl side chains. The conjugated linkers can be inserted between the electron-donating block and the acceptor unit in a donor-acceptor (D-A) molecule, and are considered to play an important role in determining energy levels, optical absorption and charge transfer properties of small molecules for high-performance OSCs. Different aromatic groups such as benzene, pyrrole, furan, thiophene, and selenophene have been widely used as conjugated linkers in organic dyes.[10] Yet the effects of linkers on the properties of conjugated molecules used in BHJ OSCs are not well understood. Herein, we have designed and synthesized a series of solution processable small molecules using sexithiophene and electron-withdrawing octyl cyanoacetate groups as building blocks and the five-membered ring heterocyclic molecules – furan, thiophene and selenophene as linkers (T1, T2, and T3, **Scheme 1**). We investigated the correlation between the molecular structures and their properties. In this work, the four octyl side-chain positions and spacing in the sexithiophene backbone, coupled with the end-capping ester group, are expected to benefit both solubility in organic solvents and miscibility with fullerene derivatives. Combining advantages of both electron linker and side chain design, we demonstrated FF well above 60% from solution processed OSC devices. A PCE of 6.15% combined with a high V_{oc} of 0.85 V, a current density (J_{sc}) of 10.79 mA cm^{-2} and a notable FF of 67.1% were obtained by using a blend of T3 and [6,6]-Phenyl C_{71} butyric acid methyl ester ($PC_{71}BM$) at a weight ratio of 1:1.2 as the active layer with polydimethylsiloxane (PDMS) as additive. Our results indicate that the electron linkers with different electron donating and polarization properties pave an effective way towards high performance of small molecule OSCs.

Dr. Y. Liu, Y. (Michael) Yang, C.-C. Chen, Dr. Q. Chen, L. Dou, Dr. Z. Hong, Dr. G. Li, Prof. Y. Yang
Department of Materials Science and Engineering
University of California
Los Angeles, California 90095, USA
E-mail: yangy@ucla.edu
Dr. Y. Liu, Dr. Q. Chen, L. Dou, Prof. Y. Yang
California Nano Systems Institute
University of California
Los Angeles, CA 90095, USA

DOI: 10.1002/adma.201301716

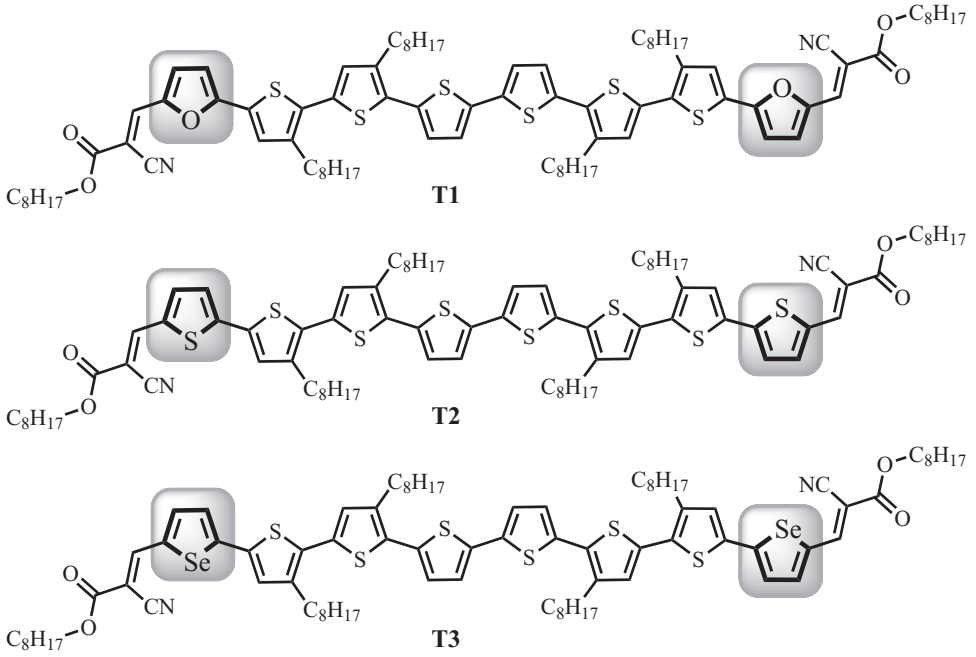

Scheme 1. Structures of T1, T2 and T3.

The syntheses of T1, T2 and T3 are outlined in **Scheme 2**. Compounds **1** and **2** were synthesized via published methods.[11] Bis(trimethylstannyl)-sexithiophene **2** was prepared via a modified route from the reported procedures.[12] 6T, containing dicarbaldehyde compounds **3, 4,** and **5**, was synthesized via Stille coupling between **2** with 5-bromo-2-formylfuran, 5-bromo-2-formylthiophene and 5-bromo-2-formylselenophene, respectively, in refluxing toluene/DMF in the presence of $Pd(PPh_3)_4$ as the catalyst in Ar atmosphere for 24 h. The targeted small molecules, T1, T2, and T3, were obtained using a Knoevenagel condensation of octyl cyanoacetate with the corresponding aldehydes. TGA analysis (Figure S1, Supporting Information) revealed that all these molecules show high thermal stability greater than 360 °C under Ar. The onset degradation temperature of these conjugated molecules is 363 °C for T1, 366 °C for T2 and 374 °C for T3. Obviously, the thermal stability of these small molecules is adequate for their applications in OSCs. Differential scanning calorimetry (DSC) analysis (Figure S2) revealed different melting peaks of 141, 148 and 151 °C for T1, T2 and T3, respectively.

The normalized absorption spectra of T1, T2 and T3 in $CHCl_3$ solution and solid film are displayed in **Figure 1**, and the corresponding data are presented in Table S1. The small molecule T1 with furan as a linker in $CHCl_3$ solution shows

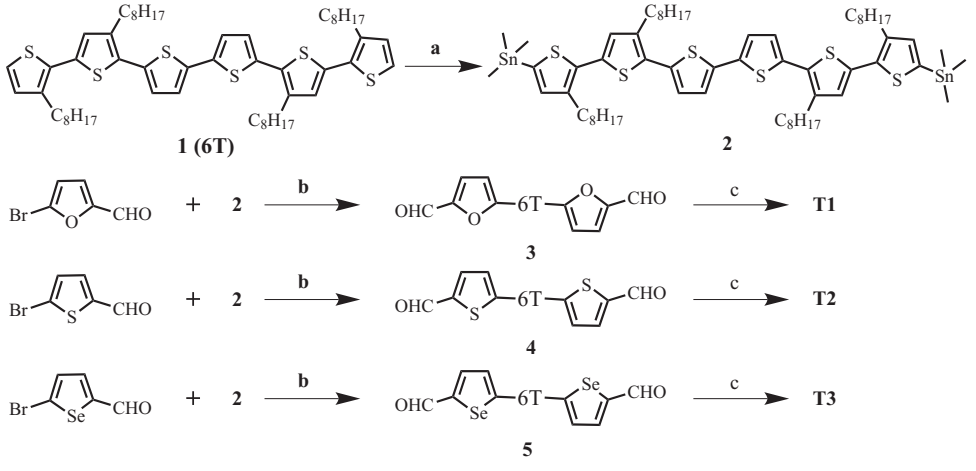

Scheme 2. Synthesis routes to T1, T2 and T3. Reagents and conditions: (a) (i) n-BuLi, (ii) $SnMe_3Cl$; (b) $Pd(PPh_3)_4$, $PhCH_3$, DMF; (c) Octyl cyanoacetate, NEt_3, $CHCl_3$.

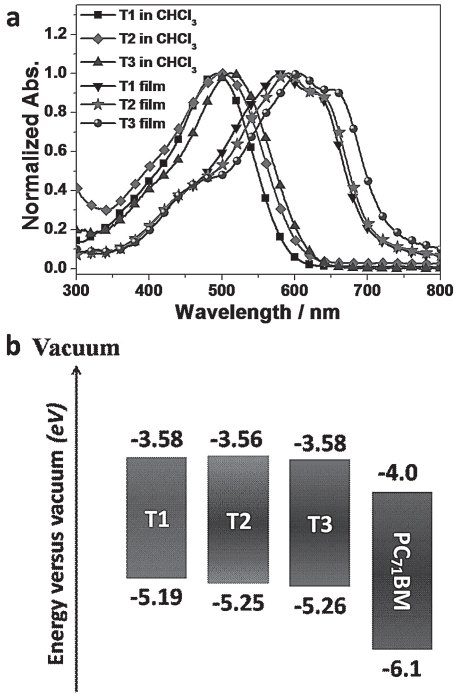

Figure 1. (a) Absorption spectra of T1, T2 and T3 in $CHCl_3$ solution and in solid film. (b) Energy levels of T1, T2, T3 and $PC_{71}BM$.

an absorption peak at 493 nm and a FWHM (full width at half maximum) of 137 nm. After replacing the linker with thiophene, the T2 solution presents a red shifted absorption peak at 501 nm and a broadened FWHM of 168 nm. A further red shift of the absorption band to 513 nm was observed for T3 with selenophene as linker, combined with a FWHM of 148 nm. Similarly, as shown in Figure 1, absorption spectra of thin films show obvious broadening (FWHM of 185 nm for T1, 183 nm for T2 and 186 nm for T3) and large red shift (87 nm for T1, 90 nm for T2 and 93 nm for T3) of the bands compared to those in solution phase. Absorption maxima of films of these conjugated molecules are located at 580 nm for T1, 591 nm for T2 and 606 nm for T3. All the films show strong sub/shoulder peak structure (626 nm for T1, 635 nm for T2, 653 nm for T3) at longer wavelength, suggesting a vibronic progression due to a rigid co-planarization of the conjugated systems enforced by molecular packing. The optical band gaps of these conjugated small molecules in thin films were estimated from the onset of the band edge absorption and found to be 1.78, 1.77 and 1.72 eV, respectively. The results show that the optical band gaps decrease with decreased electronegativity of the heteroatoms in the linkers. In comparison with T1 and T2, T3 with selenophene as a linker has a lower bandgap due to its larger π-overlap of the larger p-orbitals of selenium atoms and the intermolecular Se–Se interactions. Such strong intermolecular interaction should improve the packing structure of T3 in solid state and facilitate intermolecular charge transfer. The HOMO and LUMO energy levels of these small molecules were measured by cyclic voltammetry (Figure S3). The energy levels of the HOMO and LUMO, which are − 5.19 and − 3.58 eV for T1, − 5.25 and − 3.56 eV for T2, and − 5.26 and − 3.58 eV for T3, were calculated from the onset oxidation potentials and the onset reduction potentials.[13]

Hole mobilities of the pristine small molecules were measured in a device structure of ITO/PEDOT:PSS/small molecule/Au. *J–V* characteristics are plotted in Figure S8. By fitting the *J–V* curves to the space charge limited current (SCLC) model, the hole mobilities were estimated to be 1.1×10^{-4} cm^2 V^{-1} s^{-1} for T1, 1.2×10^{-4} cm^2 V^{-1} s^{-1} for T2 and 1.6×10^{-4} cm^2 V^{-1} s^{-1} for T3. These mobility values are similar to that of the recently reported small molecule material DCAO7T (3.26×10^{-4} cm^2 V^{-1} s^{-1}).[14]

From the X-ray diffraction (XRD) patterns presented in **Figure 2**, the crystalline nature of these small molecules in the spin-coated film are evident and detailed *d*-spacing values are summarized in Table S3. XRD of a blend film of these small molecules with $PC_{71}BM$ were also carried out to investigate the changes induced in the small molecule crystalline structure upon the addition of $PC_{71}BM$ (Figure S4) and detailed *d*-spacing values are summarized in Table S3. As shown in Figure 2a, the three π-conjugated molecules exhibited strong (100) reflection peaks at $2\theta = 5.02°$ for T1, 5.17° for T2 and 5.20° for T3, corresponding to d_{100}–spacing values of 17.6, 17.1 and 17.0 Å, respectively. These d_{100}–spacing values are the distance of the main conjugation chains of these molecules separated by

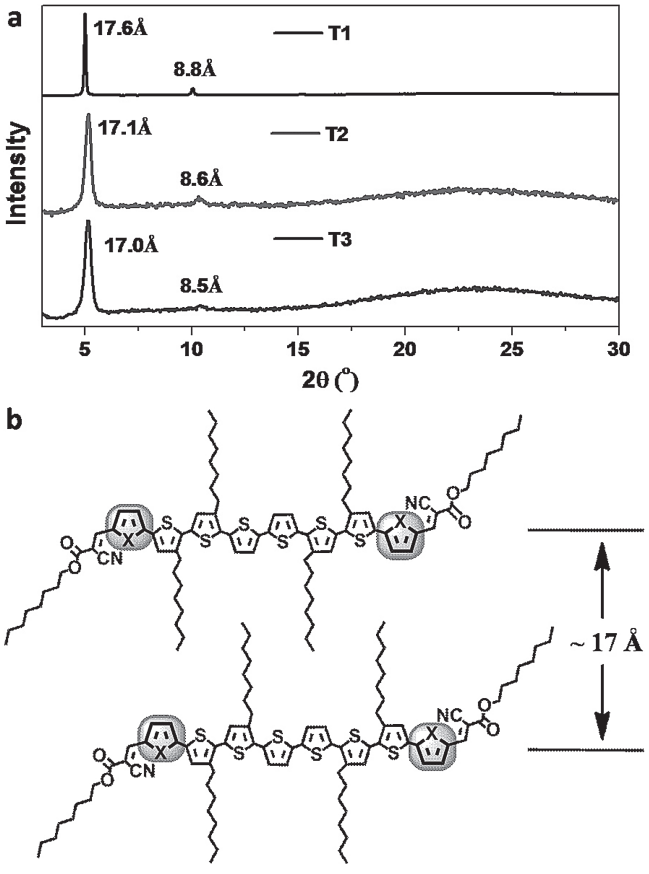

Figure 2. (a) XRD patterns of T1, T2 and T3 films spin-coated from $CHCl_3$ on glass substrates. (b) Proposed packing structures of T1, T2, and T3 (X = O, S, or Se).

Table 1. OPV performance of T1/$PC_{71}BM$, T2/$PC_{71}BM$ and T3/$PC_{71}BM$ based devices with a weight blend ratio of 1:1.2.

	V_{oc} (V)	J_{sc} (mA cm^{-2})	PCE (%)	FF (%)
T1/$PC_{71}BM$	0.78	6.34	3.18	64.3
T2/$PC_{71}BM$	0.85	7.43	4.52	71.6
T3/$PC_{71}BM$	0.85	8.99	5.04	66.0
T3/$PC_{71}BM$[a)]	0.85	10.79	6.15	67.1

[a)] PDMS as additive (0.1 mg mL^{-1}).

alkyl side chains. Compared to DCAO7T (21.0 Å)[14] and P3OT (20.1 Å),[15] the d_{100}-spacing values of T1, T2 and T3 decrease about 3 Å. Because the length of the octyl group is about 9.3 Å, d_{100}-spacing values of T1, T2 and T3 are shorter than two times the length of octyl group, thus partial interdigitated alkyl chains structures should occur (Figure 2b). This indicates that the structural order of these small molecules was increased compared with DCAO7T and P3OT, even though the same octyl side chains were used. DeLongchamp et al. suggested that side chain interdigitation of conjugated polymers provides a three dimensional chain ordering, and results in high charge transporting properties.[16] In our case, we also expect that the partial interdigitated alkyl chains structures of these conjugated molecules should benefit charge transport in the device. The second-order diffraction peaks (200) of these conjugated molecules were also clearly observed, which are attributed to the formation of lamellar structures, implying a highly organized assembly of these small molecules in solid state. As shown in Figure S4, similar (100) reflection peaks are observed from the blend films, while (200) reflection peaks are weak. It indicates that the addition of $PC_{71}BM$ has no strong influence on the lamellar structures formed by the conjugated molecules.

To investigate the photovoltaic properties of the three small molecules, bulk heterojunction (BHJ) solar cells with a device structure of ITO/PEDOT:PSS/donor:$PC_{71}BM$/Ca/Al were fabricated. The photovoltaic properties of the devices fabricated under optimal conditions are listed in **Table 1** and the corresponding current-density versus voltage (*J–V*) curves of these devices are shown in **Figure 3**. The most efficient photovoltaic cells were obtained from the BHJ systems made using T1, T2 or T3 with $PC_{71}BM$, which were optimized at a weight ratio of 1:1.2. A device with T1 as donor showed a PCE of 3.18%, with a J_{sc} of 6.34 mA cm^{-2}, a V_{oc} of 0.78 V and an FF of 64.3%. The lower V_{oc} agrees with its high-lying HOMO level. The PCE of a T2/$PC_{71}BM$ based device reached 4.52% with a large V_{oc} of 0.85 V, a J_{sc} of 7.43 and a FF of 71.6%. The good photovoltaic performance of T2 could be partially ascribed to its better spectral coverage and low-lying HOMO level. Combined with a V_{oc} of 0.85 V, an FF of 66.0% and a higher J_{sc} of 8.99 mA cm^{-2}, T3 based devices yield a PCE as high as 5.04%, showing nearly a 12% increase compared with that of T2. The higher *Jsc* could be ascribed to the better solar spectral coverage of T3, which red shifts by ≈15 nm in λ_{max} as compared with that of T2. Thus, the improved photovoltaic efficiency of T3 should stem from the highly ordered molecular packing, which is expected to result in the enhanced hole mobility and broader absorption. The low

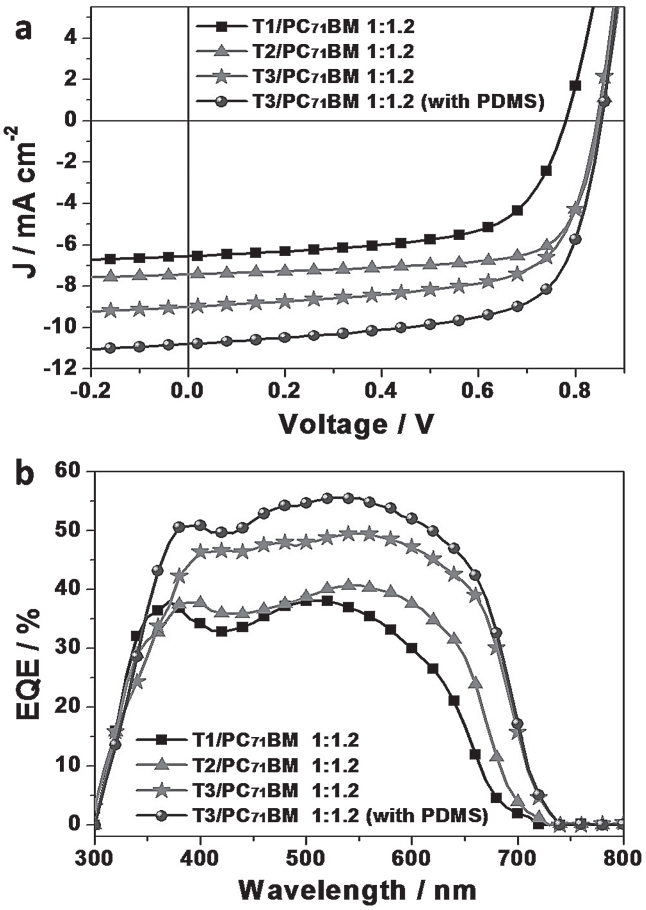

Figure 3. (a) *J-V* curves of BHJ OSCs based on T1/$PC_{71}BM$ (1:1.2, w/w), T2/$PC_{71}BM$ (1:1.2, w/w) and T3/$PC_{71}BM$ (1:1.2, w/w) without PDMS, and T3/$PC_{71}BM$ (1:1.2, w/w) with 0.1 mg mL^{-1} PDMS as additive. (b) EQE curves of the corresponding BHJ OSCs.

PCE of T1 on the other side, could be related to its low hole mobility and narrowed absorption (26 nm blue shift in λ_{max} compared with that of T3). After replacing the thiophene linker (in T2) with the selenophene linker, T3 shows a broad absorption and lower band gap. It is interesting to note that the device based on T3 still maintains the same V_{oc} as that of the device based on T2. This result is also consistent with their similar HOMO energy levels.

Due to the promising photovoltaic properties of T3, we further optimized the device through morphology control. By adding a small amount of a macromolecular additive (PDMS), which has been shown to be a good additive in small molecule OSCs,[4c,17] in the active layer, we were able to further improve the efficiency. The effect of different concentrations of PDMS in the active layer solution on the device performance was studied. The OSCs based on T3/$PC_{71}BM$ with 0.1 mg mL^{-1} PDMS additive reached a high PCE of 6.15%, with a V_{oc} of 0.85 V, a J_{sc} of 10.79 mA cm^{-2}, and a notable FF of 67.1%. This is more than 20% increase in J_{sc} and 22% increase in PCE over the device without PDMS. The better performance of the device after adding PDMS is mainly due to the enhanced J_{sc}, which could be ascribed to a better photo-to-current response

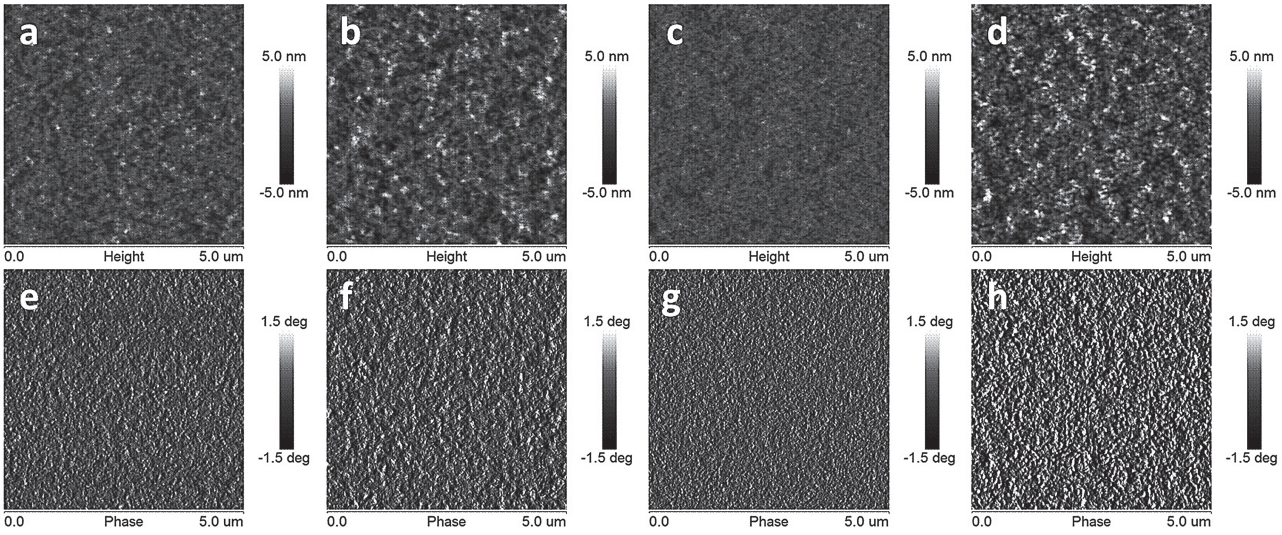

Figure 4. Tapping-mode AFM height (top) and phase (down) images (5 × 5 μm) of blend films (w/w: 1:1.2) spin-coated from chloroform solutions on glass/ITO/PEDOT:PSS substrates. (a,e) Blend film of T1/$PC_{71}BM$. (b,f) Blend film of T2/$PC_{71}BM$. (c,g) Blend film of T3/$PC_{71}BM$. (d,h) Blend film of T3/$PC_{71}BM$ with PDMS (0.1 mg mL^{-1}) as additive.

(maximum EQE: 50% to 56%) and efficient exciton dissociation as discussed below.

The EQE curves of the corresponding BHJ devices are shown in Figure 3b. J_{sc} values were calculated from the integral of the EQE curves over the AM1.5G solar spectrum and are summarized in Table S7. The difference in J_{sc} values of these small molecule based devices seen in the *J-V* curves are further reflected in the EQE spectra. As shown in Figure 3b, the EQE of the T3 based devices shows a broader and higher photon-to-current response than that of the T1 and T2 based devices. Compared with the T2 based device, the BHJ device using T3 as donor material leads to approximate 22% enhancement in EQE across the wavelength region from 350 to 700 nm. This result proves that the conjugated molecule using selenophene as a linker is not only capable of broadening the solar spectral coverage, but also of improving the photo-to-current response. With PDMS as a processing additive, the EQE of the T3/$PC_{71}BM$ based devices was enhanced in the entire photoresponse range from 300 to 730 nm, and reached a maximum of 56% at 530 nm. The addition of PDMS leads to ≈20% enhancement in J_{sc} and EQE, clearly indicating that the PDMS additive plays a positive role in morphology control via optimizing phase separation in the BHJ films. That means the additive helps to form interdigitated donor/acceptor networks with suitable crystal size for exciton dissociation, as observed from transmission electron microscopy (TEM) images (Figure S10) and atomic force microscopy (AFM) images below. Therefore, the photocurrent is significantly enhanced.

Tapping-mode AFM was employed to characterize the surface morphology of the active laver. The tapping-mode AFM height and phase images of small molecules/$PC_{71}BM$ (w:w, 1:1.2) blend films are shown in **Figure 4**. The different root mean square (RMS) roughness suggests a variation in surface morphology for these blend films. The films in Figure 4 have a RMS roughness of 0.699 nm for T1/$PC_{71}BM$, 0.996 nm for T2/$PC_{71}BM$, and 0.545 nm for T3/$PC_{71}BM$, respectively. The low RMS roughness of these blend films indicate that these donor materials have good miscibility with $PC_{71}BM$ molecules in the blend films, and may form a finer interpenetrating network, which facilitates both exciton separation and charge transport. Compared to the pristine T3/$PC_{71}BM$ film, the additive processed film, however, showed a slightly larger surface roughness (Ra = 1.17 nm) presumably due to the higher degree of T3 and $PC_{71}BM$ aggregation, which can also be seen from the TEM images (Figure S10), resulting in more favorable donor/acceptor phase separation for efficient charge separation and transport.[18] The RMS values coincide with the FF of these small molecule based devices, meaning that aggregation of $PC_{71}BM$ occurs and favors electron transport. As shown in Figure 4, interpenetrating networks can be seen from the phase images, which indicate that well-defined nanoscale phase separation and efficient percolation channels have been formed, thus benefiting the exciton dissociation at the small molecule/$PC_{71}BM$ interfaces and facilitating efficient charge carrier transport to the electrodes, leading to high FF and optimal device performance.

In conclusion, we have designed and synthesized a class of solution processable small molecules using furan, thiophene and selenophene as electron linkers for application in BHJ OSCs. We show that the variation of the electron linkers enables fine-tuning of the optical energy gap as well as of the HOMO and LUMO levels. All these small molecules show high PCEs, ranging from 3.18–6.15% under simulated AM 1.5G condition (100 mW cm^{-2}), and the highest PCE of 6.15% was achieved for a T3/$PC_{71}BM$ (w:w, 1:1.2) based device using PDMS as additive, giving a high V_{oc} of 0.85 V, a J_{sc} of 10.79 mA cm^{-2} and a notable FF of 67.1%. Our results indicate that the optoelectronic properties of semiconductive oligomers can be easily manipulated by introducing different electron linkers, and that selenophene is a promising linker in constructing donor materials for high efficiency OSCs.

Experimental Section

Materials: All reactions and manipulations were carried out under argon atmosphere with the use of standard Schlenk techniques. All starting materials were purchased from commercial suppliers and used without further purification. 3,4' 3"",3""'-tetraoctyl-2,2':5',2":5",2"':5"',2"":5"",2""'-sexithiophene (**6T**) (**1**) was synthesized according to the literature methods.[11] Bis(trimethylstannyl)-sexithiophene **2** was prepared via a modified route from the reported procedures.[12] The targeted small molecules T1, T2, and T3, were synthesized using Knoevenagel condensation of octyl cyanoacetate with the corresponding aldehydes. See supporting information for more synthetic details.

Device Fabrication: The photovoltaic devices were made with the following structure: glass/ITO/PEDOT:PSS/donor:acceptor/Ca/Al. The ITO-coated glass substrates were cleaned by ultrasonic treatment in isopropyl alcohol, detergent, deionized water, acetone, and isopropyl alcohol under ultrasonication for 20 minutes each and subsequently dried in an oven for 12 hours. A thin layer of PEDOT:PSS (Baytron P VP AI 4083, filtered at 0.2 μm) was spin-coated (4000 rpm, ca. 40 nm thick) onto the ITO surface. After being baked at 120 °C for 15 min, the substrates were transferred into a nitrogen-filled glove box. Subsequently, the active layer was spin-coated from different blend ratios (weight-to-weight, w/w) of donor (14 mg mL^{-1}) and $PC_{71}BM$ in chloroform solution onto the ITO/PEDOT:PSS substrate without further special treatments. For the active layers fabricated with PDMS additive, PDMS with desired amounts was added in the donor/$PC_{71}BM$ blend solutions and stirred for 1 h before spin-coating. The active layer thickness was measured as ca. 120–130 nm using a Dektak 150 profilometer. Finally, a 20 nm Ca layer and a 100 nm Al layer were sequently deposited onto the active layer under high vacuum ($\approx 2 \times 10^{-5}$ Torr). The effective area of each cell was 0.1 cm^2 defined by masks for all the solar cell devices discussed in this work. See supporting information for more device fabrication and characterization details.

Supporting Information

Supporting Information is available from the Wiley Online Library or from the author.

Acknowledgements

The authors gratefully acknowledge financial support from the Office of Naval Research (Grant No. N000141110250). The authors would like to thank Mr. Wenbing Yang for assistance with the TGA and DSC measurements and Mr. Eric Richard for helpful discussion and proof reading of this manuscript. We also acknowledge the use of the Nano and Pico Characterization Lab at the California NanoSystems Institute for AFM and TEM analysis.

Received: April 17, 2013
Revised: May 17, 2013
Published online: July 4, 2013

[1] a) G. Li, V. Shrotriya, J. S. Huang, Y. Yao, T. Moriarty, K. Emery, Y. Yang, *Nat. Mater.* **2005**, *4*, 864; b) G. Li, R. Zhu, Y. Yang, *Nat. Photonics* **2012**, *6*, 153; c) M. Kaltenbrunner, M. S. White, E. D. Glowacki, T. Sekitani, T. Someya, N. S. Sariciftci, S. Bauer, *Nat. Commun.* **2012**, *3*, 770; d) P. Kumar, S. Chand, *Prog. Photovoltaics* **2012**, *20*, 377.

[2] a) Z. C. He, C. M. Zhong, S. J. Su, M. Xu, H. B. Wu, Y. Cao, *Nat. Photonics* **2012**, *6*, 591; b) Y. W. Su, S. C. Lan, K. H. Wei, *Mater. Today* **2012**, *15*, 554; c) J. B. You, L. T. Dou, K. Yoshimura, T. Kato, K. Ohya, T. Moriarty, K. Emery, C. C. Chen, J. Gao, G. Li, Y. Yang, *Nat. Commun.* **2013**, *4*, 1446.

[3] a) Y. Z. Lin, Y. F. Li, X. W. Zhan, *Chem. Soc. Rev.* **2012**, *41*, 4245; b) A. Mishra, P. Bauerle, *Angew. Chem. Int. Edit.* **2012**, *51*, 2020; c) B. Walker, C. Kim, T. Q. Nguyen, *Chem. Mater.* **2011**, *23*, 470; d) F. Wurthner, K. Meerholz, *Chem-Eur. J.* **2010**, *16*, 9366; e) O. P. Lee, A. T. Yiu, P. M. Beaujuge, C. H. Woo, T. W. Holcombe, J. E. Millstone, J. D. Douglas, M. S. Chen, J. M. J. Frechet, *Adv. Mater.* **2011**, *23*, 5359; f) H. X. Shang, H. J. Fan, Y. Liu, W. P. Hu, Y. F. Li, X. W. Zhan, *Adv. Mater.* **2011**, *23*, 1554; g) G. R. He, Z. Li, X. J. Wan, J. Y. Zhou, G. K. Long, S. Z. Zhang, M. T. Zhang, Y. S. Chen, *J. Mater. Chem. A.* **2013**, *1*, 1801.

[4] a) A. K. K. Kyaw, D. H. Wang, V. Gupta, J. Zhang, S. Chand, G. C. Bazan, A. J. Heeger, *Adv. Mater.* **2013**, 25, 2445; b) T. S. van der Poll, J. A. Love, T. Q. Nguyen, G. C. Bazan, *Adv. Mater.* **2012**, *24*, 3646; c) J. Y. Zhou, X. J. Wan, Y. S. Liu, Y. Zuo, Z. Li, G. R. He, G. K. Long, W. Ni, C. X. Li, X. C. Su, Y. S. Chen, *J. Am. Chem. Soc.* **2012**, *134*, 16345.

[5] a) H. Burckstummer, E. V. Tulyakova, M. Deppisch, M. R. Lenze, N. M. Kronenberg, M. Gsanger, M. Stolte, K. Meerholz, F. Würthner, *Angew. Chem. Int. Edit.* **2011**, *50*, 11628; b) G. Chen, H. Sasabe, Z. Q. Wang, X. F. Wang, Z. R. Hong, J. Kido, Y. Yang, *Phys. Chem. Chem. Phys.* **2012**, *14*, 14661; c) Z. Li, G. R. He, X. J. Wan, Y. S. Liu, J. Y. Zhou, G. K. Long, Y. Zuo, M. T. Zhang, Y. S. Chen, *Adv. Energy. Mater.* **2012**, *2*, 74; d) Y. S. Liu, X. J. Wan, B. Yin, J. Y. Zhou, G. K. Long, S. G. Yin, Y. S. Chen, *J. Mater. Chem.* **2010**, *20*, 2464; e) S. Loser, C. J. Bruns, H. Miyauchi, R. P. Ortiz, A. Facchetti, S. I. Stupp, T. J. Marks, *J. Am. Chem. Soc.* **2011**, *133*, 8142; f) B. Walker, A. B. Tomayo, X. D. Dang, P. Zalar, J. H. Seo, A. Garcia, M. Tantiwiwat, T. Q. Nguyen, *Adv. Funct. Mater.* **2009**, *19*, 3063.

[6] C. M. Proctor, C. Kim, D. Neher, T.-Q. Nguyen, *Adv. Funct. Mater.* **2013**, DOI: 10.1002/adfm.201202643.

[7] M. Halik, H. Klauk, U. Zschieschang, G. Schmid, W. Radlik, S. Ponomarenko, S. Kirchmeyer, W. Weber, *J. Appl. Phys.* **2003**, *93*, 2977.

[8] S. W. Ko, E. T. Hoke, L. Pandey, S. H. Hong, R. Mondal, C. Risko, Y. P. Yi, R. Noriega, M. D. McGehee, J. L. Bredas, A. Salleo, Z. A. Bao, *J. Am. Chem. Soc.* **2012**, *134*, 5222.

[9] G. Sauve, A. E. Javier, R. Zhang, J. Y. Liu, S. A. Sydlik, T. Kowalewski, R. D. McCullough, *J. Mater. Chem.* **2010**, *20*, 3195.

[10] a) H. Y. Chen, S. C. Yeh, C. T. Chen, C. T. Chen, *J. Mater. Chem.* **2012**, *22*, 21549; b) Z. Q. Wan, C. Y. Jia, Y. D. Duan, L. L. Zhou, Y. Lin, Y. Shi, *J. Mater. Chem.* **2012**, *22*, 25140; c) J. B. Yang, F. L. Guo, J. L. Hua, X. Li, W. J. Wu, Y. Qu, H. Tian, *J. Mater. Chem.* **2012**, *22*, 24356.

[11] a) Y. S. Liu, J. Y. Zhou, X. J. Wan, Y. S. Chen, *Tetrahedron* **2009**, *65*, 5209; b) H. Nakanishi, N. Sumi, Y. Aso, T. Otsubo, *J. Org. Chem.* **1998**, *63*, 8632.

[12] M. Endou, Y. Ie, T. Kaneda, Y. Aso, *J. Org. Chem.* **2007**, *72*, 2659.

[13] L. T. Dou, J. Gao, E. Richard, J. B. You, C. C. Chen, K. C. Cha, Y. J. He, G. Li, Y. Yang, *J. Am. Chem. Soc.* **2012**, *134*, 10071.

[14] Y. S. Liu, X. J. Wan, F. Wang, J. Y. Zhou, G. K. Long, J. G. Tian, J. B. You, Y. Yang, Y. S. Chen, *Adv. Energy. Mater.* **2011**, *1*, 771.

[15] T. A. Chen, X. M. Wu, R. D. Rieke, *J. Am. Chem. Soc.* **1995**, *117*, 233.

[16] R. J. Kline, D. M. DeLongchamp, D. A. Fischer, E. K. Lin, L. J. Richter, M. L. Chabinyc, M. F. Toney, M. Heeney, I. McCulloch, *Macromolecules* **2007**, *40*, 7960.

[17] K. R. Graham, J. G. Mei, R. Stalder, J. W. Shim, H. Cheun, F. Steffy, F. So, B. Kippelen, J. R. Reynolds, *Acs. Appl. Mater. Inter.* **2011**, *3*, 1210.

[18] a) J. K. Lee, W. L. Ma, C. J. Brabec, J. Yuen, J. S. Moon, J. Y. Kim, K. Lee, G. C. Bazan, A. J. Heeger, *J. Am. Chem. Soc.* **2008**, *130*, 3619; b) Y. Zhang, J. Y. Zou, H. L. Yip, K. S. Chen, J. A. Davies, Y. Sun, A. K. Y. Jen, *Macromolecules* **2011**, *44*, 4752.